TOAC Spin Labels in the Backbone of Alamethicin: EPR Studies in Lipid Membranes

Derek Marsh,* Micha Jost,† Cristina Peggion,† and Claudio Toniolo†
*Max-Planck-Institut für biophysikalische Chemie, Abteilung Spektroskopie, Göttingen, Germany; and †Department of Chemistry, University of Padova, Padova, Italy

ABSTRACT Alamethicin is a 19-amino-acid residue hydrophobic peptide that produces voltage-dependent ion channels in membranes. Analogues of the Glu(OMe)^{7,18,19} variant of alamethicin F50/5 that are rigidly spin-labeled in the peptide backbone have been synthesized by replacing residue 1, 8, or 16 with 2,2,6,6-tetramethyl-piperidine-1-oxyl-4-amino-4-carboxyl (TOAC), a helicogenic nitroxyl amino acid. Conventional electron paramagnetic resonance spectra are used to determine the insertion and orientation of the TOAC^n alamethicins in fluid lipid bilayer membranes of dimyristoyl phosphatidylcholine. Isotropic ^{14}N-hyperfine couplings indicate that TOAC^8 and TOAC^{16} are situated in the hydrophobic core of the membrane, whereas the TOAC^1 label resides closer to the membrane surface. Anisotropic hyperfine splittings show that alamethicin is highly ordered in the fluid membranes. Experiments with aligned membranes demonstrate that the principal diffusion axis lies close to the membrane normal, corresponding to a transmembrane orientation. Combination of data from the three spin-labeled positions yields both the dynamic order parameter of the peptide backbone and the intramolecular orientations of the TOAC groups. The latter are compared with x-ray diffraction results from alamethicin crystals. Saturation transfer electron paramagnetic resonance, which is sensitive to microsecond rotational motion, reveals that overall rotation of alamethicin is fast in fluid membranes, with effective correlation times $<$30 ns. Thus, alamethicin does not form large stable aggregates in fluid membranes, and ionic conductance must arise from transient or voltage-induced associations.

INTRODUCTION

Alamethicin is a 19-amino-acid residue peptide from *Trichoderma viride* (with an N-terminal acetyl and a C-terminal phenylalaninol) that is able to induce voltage-dependent ion conduction across lipid membranes (1,2). The channel properties are strongly concentration-dependent and characterized by multiple conduction states (3). Mechanistic studies suggest that consecutive conductance levels are generated by incorporation of single alamethicin molecules into an existing pore aggregate (4). The relative populations of the different conductance levels are responsive to membrane tension and to the intrinsic curvature of the constituent lipids (5,6).

TOAC is a helicogenic nitroxyl amino acid that can be incorporated directly in the backbone of synthetic peptides (7–10). The nitroxide ring is rigidly attached to the C^{α}-atom of the amino acid and therefore can be used as a spin-label reporter of the orientation and dynamics of the peptide backbone (11). Previous studies have demonstrated the utility of conventional electron paramagnetic resonance (EPR) spectroscopy to determine the location and orientation of TOAC-labeled trichogin GA IV, a membrane-active peptide, in lipid bilayers (12). Such methods exploit both the polarity sensitivity (13) and the angular dependence (14) of the nitroxide EPR spectra.

In this work, we investigate the association of TOAC-labeled alamethicin analogs with phospholipid bilayer membranes by using both conventional and saturation-transfer (ST-) EPR spectroscopy. The TOAC residue is substituted at one of three positions (1, 8, or 16) throughout the sequence of alamethicin. Macroscopically aligned membranes are used to demonstrate that the TOAC-labeled alamethicin assumes a transmembrane orientation, consistent with the relative environmental polarities of the different TOAC positions. Orientational order parameters for the three TOAC positions allow determination of both the angular amplitude of long-axis motion and the intramolecular tilts of the individual nitroxides. Finally, ST-EPR, which is sensitive to much slower rotational diffusion than conventional EPR (15), and the lack of spin-spin interactions between monomers in the conventional EPR, are used to obtain information on the aggregation state of the peptide in the membrane.

MATERIALS AND METHODS

Materials

Dimyristoyl phosphatidylcholine (DMPC) was from Avanti Polar Lipids (Alabaster, AL). Spin-labeled derivatives of alamethicin F50/5 [TOAC^n, Glu(OMe)^{7,18,19}], with $n = 1$, 8, and 16, were synthesized according to references (16,17). The complete amino-acid sequences of the three analogs are:

Submitted July 4, 2006, and accepted for publication September 14, 2006.

Address reprint requests to Dr. Derek Marsh, Tel.: 49-551-201-1285; E-mail: dmarsh@gwdg.de.

Abbreviations used: Ac, acetyl; Aib, α-aminoisobutyric acid; DMPC, 1,2-dimyristoyl-*sn*-glycero-3-phosphocholine; EDTA, *N*,*N*,*N*′,*N*′-ethylenediaminetetraacetic acid; EPR, electron paramagnetic resonance; Hepes, *N*-(2-hydroxyethyl)piperazine-*N*′-2-ethanesulphonic acid; NH*t*Bu, *tert*-butylamino; OMe, methoxy; Phol, phenylalaninol; ST-EPR, saturation transfer EPR; TOAC, 2,2,4,4-tetramethylpiperidine-1-oxy-4-amino-4-carboxylic acid; V_1, first-harmonic absorption EPR spectrum detected in phase with respect to the static magnetic field modulation; V_2', second-harmonic absorption EPR spectrum detected 90° out-of-phase with respect to the static magnetic field modulation; *Z*, benzyloxycarbonyl.

0006-3495/07/01/473/09 $2.00

doi: 10.1529/biophysj.106.092775

Ac-TOAC-Pro-Aib-Ala-Aib-Ala-Glu(OMe)-Aib-Val-Aib-Gly-Leu-Aib-Pro-Val-Aib-Aib-Glu(OMe)-Glu(OMe)-Phol [TOAC^{1},Glu(OMe)^{7,18,19}]
Ac-Aib-Pro-Aib-Ala-Aib-Ala-Glu(OMe)-TOAC-Val-Aib-Gly-Leu-Aib-Pro-Val-Aib-Aib-Glu(OMe)-Glu(OMe)-Phol [TOAC^{8},Glu(OMe)^{7,18,19}]
Ac-Aib-Pro-Aib-Ala-Aib-Ala-Glu(OMe)-Aib-Val-Aib-Gly-Leu-Aib-Pro-Val-TOAC-Aib-Glu(OMe)-Glu(OMe)-Phol [TOAC^{16},Glu(OMe)^{7,18,19}],

where Aib is α-aminoisobutyric acid and Phol is the β-amino alcohol L-phenylalaninol. Functional measurements demonstrate that the Gln^{7,18,19} to Glu(OMe)^{7,18,19} substitution in F50/5 alamethicin does not dramatically reduce the voltage-dependent membrane conductance that is induced by this channel-forming peptide (18).

Sample preparation

DMPC (1 mg) and ~1 mol % of the desired TOAC spin-labeled alamethicin (in MeOH) were codissolved in CH_2Cl_2, and the solution then evaporated with dry nitrogen. After keeping under vacuum overnight, the dry mixture was hydrated in 50 μl of 10 mM Hepes (*N*-(2-hydroxyethyl)piperazine-*N*′-2-ethanesulphonic acid), 10 mM NaCl, 10 mM EDTA (*N*,*N*,*N*′,*N*′-ethyle nediaminetetraacetic acid), pH 7.8 buffer, with vortex mixing at 37°C. The lipid dispersion was then transferred to a 1 mm-diameter glass capillary and pelleted in a benchtop centrifuge. Excess supernatant was removed and the capillaries were flame-sealed.

Aligned planar phospholipid bilayers were formed by evaporating the CH_2Cl_2 solution of DMPC plus 1 mol % of TOAC-alamethicin onto the internal faces of a quartz flat cell (Wilmad model No. WG-812, Wilmad-LabGlass, Buena, NJ) by using a stream of dry nitrogen. Residual solvent was removed under vacuum overnight. The oriented lipid film was hydrated with excess buffer containing 150 mM NaCl, at room temperature. The cells were drained and sealed immediately before measurement, with sufficient buffer retained to ensure complete hydration throughout the experiment.

EPR spectroscopy

EPR spectra were recorded on a Varian Century-Line 9-GHz spectrometer (Varian, Palo Alto, CA) with 100 kHz field modulation. Sample capillaries were accommodated in standard quartz EPR tubes that contained light silicone oil for thermal stability. Temperature was regulated by thermostated nitrogen gas-flow through a quartz Dewar, and was measured with a fine-wire thermocouple situated in the silicone oil at the top of the microwave cavity. Samples of ~5-mm height were centered in the rectangular TE_{102} resonator, to minimize microwave- and modulation-field inhomogeneities (19). The microwave H_1-field at the sample was measured as described in the latter reference. Conventional EPR spectra were recorded in the in-phase first-harmonic absorption mode (V_1-display), and saturation transfer (ST-) EPR spectra in the out-of-phase second-harmonic absorption mode (V_2'-display) (20). Oriented bilayer spectra were obtained with the quartz flat cells in a TE_{102} rectangular microwave cavity mounted with its H_1-field axis horizontal. The entire cavity assembly was thermostated with nitrogen gas-flow.

Conventional EPR spectra were analyzed in terms of the outer and inner hyperfine splittings, $2A_{max}$ and $2A_{min}$, respectively. The outer hyperfine splitting is a useful empirical measure of the chain dynamics and ordering that is valid in both slow and fast motional regimes of nitroxide EPR spectroscopy (21,22). In the motional narrowing regime, at high temperature, A_{max} is equal to the parallel element, $A_{//}$, of the partially motionally averaged, axial hyperfine tensor. The perpendicular element, $A_{\perp}$, is derived from the separation, $2A_{min}$, of the inner extrema (23):

$$A_{\perp}(Gauss) = A_{min} + 1.32 + 1.86\times \log_{10}(1 - S_{app}) \quad \text{for } S_{app}^3 \geq 0.45 \tag{1}$$

and

$$A_{\perp}(Gauss) = A_{min} + 0.85 \text{ for } S_{app} < 0.45, \tag{2}$$

where $S_{app} = (A_{max} - A_{min})/[A_{zz} - \frac{1}{2}(A_{xx} + A_{yy})]$ for a spin-label hyperfine tensor with Cartesian elements (A_{xx},A_{yy},A_{zz}). The environmental polarity was then characterized by means of the isotropic ^{14}N-hyperfine coupling, a_o (13), which is given by

$$a_o = \frac{1}{3}(A_{//} + 2A_{\perp}). \tag{3}$$

In addition, the order parameter of the spin-label *z* axis, in the fast motional regime, is given by

$$S_{zz} = \frac{A_{//} - A_{\perp}}{A_{zz} - \frac{1}{2}(A_{xx} + A_{yy})} \times \frac{A_{xx} + A_{yy} + A_{zz}}{3a_o}, \tag{4}$$

where the final factor on the right is a polarity correction to the hyperfine tensor elements. Values taken for the hyperfine tensor elements are (A_{xx},A_{yy},A_{zz}) = (6.0 G, 7.3 G, 34.5 G) from 2,2,4,4-tetramethylpiperidine-1-oxy in a toluene glass (24).

Saturation transfer EPR spectra were analyzed in terms of the diagnostic line-height ratios, L″/L, C′/C, and H″/H, defined in the low-field, central, and high-field regions of the spectra, respectively (15), and by the normalized integrated intensity, I_{ST} (25). Effective rotational correlation times, τ_R^{eff}, were obtained from ST-EPR line-height ratios, *R*, by using calibrations with spin-labeled hemoglobin in solutions of known viscosity from Horváth and Marsh (25). The calibrations can be expressed as (26)

$$\tau_R^{eff} = k/(R - R_o) - b, \tag{5}$$

where R_o is the rigid-limit value of *R*. The calibration constants *k*, *b*, and R_o are given in Marsh (27). For shorter correlation times, polynomial ST-EPR calibrations were used from Horváth and Marsh (28).

TOAC orientation

The crystal structure of the $^{6}T_2$ twist-boat conformer of TOAC was taken from molecule B of *Z*-TOAC-(L-Ala)$_2$-NH*t*Bu (29), which was obtained from the Cambridge Crystallographic Data Centre (CCDC code: 123753). In the available crystal structures of α-helical TOAC peptides, $^{6}T_2$ is by far the most prevalent conformer of TOAC (30). The crystal structure of native alamethicin (31) was obtained from the Research Collaboration for Structural Bioinformatics protein database (32) (PDB code: 1amt). The TOAC residue was substituted for the Aib residue at position 1, 8, or 16 in alamethicin by constraining the transformed coordinates of the TOAC N, C^{α} and C′ atoms to coincide with those in alamethicin, by using nonlinear least-squares optimization.

The orientation θ_z of the nitroxide *z* axis of TOAC to the alamethicin molecular axis was determined as described in Marsh (30). The molecular axis of alamethicin was taken as the axis of the longer (N-terminal) helical section. The latter was defined as the line equidistant from the C^{α} atoms of residues 4–14, for which the mean radial distance is 2.38 Å, by nonlinear least-squares fitting. The vector connecting the C^{α} atoms of residues 1 and 19 was also used as an alternative definition of the molecular axis. The unpublished structure of [TOAC^{16}, Glu(OMe)^{7,18,19}]-alamethicin (33), and variants in which the TOAC residue from position 16 was substituted for the Aib^{1} or Aib^{8} residue, were used in an analogous manner to obtain the orientation of the TOAC nitroxyl axes. This alamethicin analog has the $^{6}T_2$ twist-boat conformer of TOAC that is found in the *Z*-TOAC-(L-Ala)$_2$-NH*t*Bu reference peptide.

RESULTS AND DISCUSSION

Conventional spin-label EPR spectra

Fig. 1 shows the EPR spectra of the three different TOAC^{1}, TOAC^{8}, and TOAC^{16} analogs of [Glu(OMe)^{7,18,19}] alamethicin

in DMPC bilayer membranes. Spectra are shown at various temperatures, both above and below the lipid chain-melting temperature of 23°C. In the gel phase, the spectra are indicative of strong immobilization on the nanosecond timescale, but that of the TOAC[1] derivative also evidences strong spin-spin broadening. The latter is seen most clearly at 10°C as a strong distortion of the baseline by a very broad underlying component (*dotted-line spectrum*). This spin-spin interaction is caused by aggregation of the spin-labeled alamethicin in the gel-phase membrane. The sharp features in the low-temperature spectra most probably arise from a population of noninteracting spin labels, and therefore indicate some heterogeneity in the degree of aggregation. The aggregation observed by spin-spin interaction in the gel-phase correlates well with functional studies on the effects of the lipid chain-melting transition. The transmembrane current density mediated by alamethicin in unsupported bilayers of 1-stearoyl-3-myristoylphosphatidylcholine was found to increase dramatically on entering the gel phase of the membrane from the fluid phase (34). The current density in the gel phase at 24°C corresponded to a pore concentration of $\sim 10^6$ pores/cm^2 and decreased to a low level representing only 1 pore/cm^2 in the fluid phase. Increased pore density implies an increased degree of peptide aggregation and an increased local concentration of alamethicin in the gel phase that manifests itself here as an increase in spin-spin interactions.

Spin-spin broadening is absent from the EPR spectra in the fluid phase at 1 mol % spin label. This finding indicates that the spin-labeled alamethicin is randomly dispersed in the lipid membrane at temperatures above the lipid chain-melting transition. Similar conclusions have been reached from EPR studies on alamethicin with a flexible spin label at the N- or C-terminus (35,36). The spectra from the three TOAC derivatives are still highly anisotropic, indicating high ordering or limited motion, in the fluid phase. The extent of spectral anisotropy decreases with increasing temperature. At higher temperatures, the spectra display axial motional averaging, as indicated by the well-defined outer and inner hyperfine splittings, $2A_{max}$ and $2A_{min}$, respectively (see, e.g., (37)).

Temperature dependence

Fig. 2 shows the temperature dependence of the outer hyperfine splitting, $2A_{max}$, for alamethicin with the three different positions of TOAC labeling in DMPC membranes. For the TOAC[8] and TOAC[16] derivatives, there is a small but abrupt decrease in the value of A_{max} at the DMPC chain-melting transition. This decrease in A_{max} corresponds to an increase in rotational dynamics of alamethicin on lipid chain fluidization. The apparent increase in A_{max} for the TOAC[1] derivative at 23°C most probably is an artifact arising from the spin-spin broadening of this particular label in the gel phase. The values of A_{max} at temperatures immediately above the lipid transition are still indicative of a high degree of order, or limited amplitude of angular motion, of the spin-labeled alamethicin. There are, nonetheless, differences between the values of A_{max} and their rate of change with temperature for the three different label positions. For each label, the values of A_{max} decrease steadily in response to the increased extent of lipid chain motion with increasing temperature.

Isotropic hyperfine couplings

Fig. 3 gives the temperature dependence of the effective isotropic hyperfine couplings, a_o, defined by Eq. 3, for the different positions of TOAC labeling. The true value of a_o should depend only on the polarity of the environment in which the spin label is situated (see, e.g., (38,39)), and not on the molecular motion. Therefore, it is expected to be approximately independent of temperature. Artifactual increases in effective values with decreasing temperature are found at lower temperatures, due to the breakdown of motional narrowing theory (on which Eqs. 3 and 4 are based) caused by slow-motional contributions to the spectra at the lower temperatures. This provides a useful experimental criterion by which to define the temperature region over which motional narrowing theory is valid. Fig. 3 shows that the values of a_o are practically constant for the TOAC[1] and TOAC[8] analogs at temperatures of 55°C or higher. Only for the TOAC[16] analog is the temperature dependence

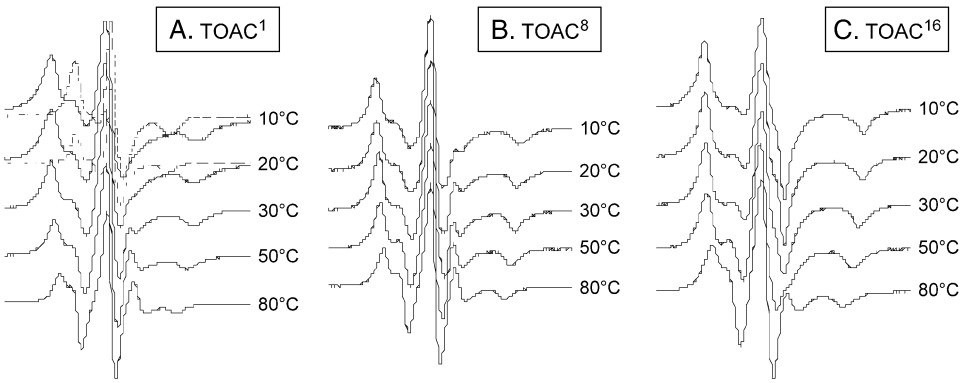

FIGURE 1 Conventional EPR spectra (V_1-display) of [Glu(OMe)^{7,18,19}] alamethicin analogs with TOAC substituted for (*A*) residue 1, TOAC[1]; (*B*) residue 8, TOAC[8]; and (*C*) residue 16, TOAC[16], in DMPC bilayers at the temperatures indicated. (*Solid lines*, total scan width = 100 Gauss; *dotted lines*, total scan width: 160 Gauss.)

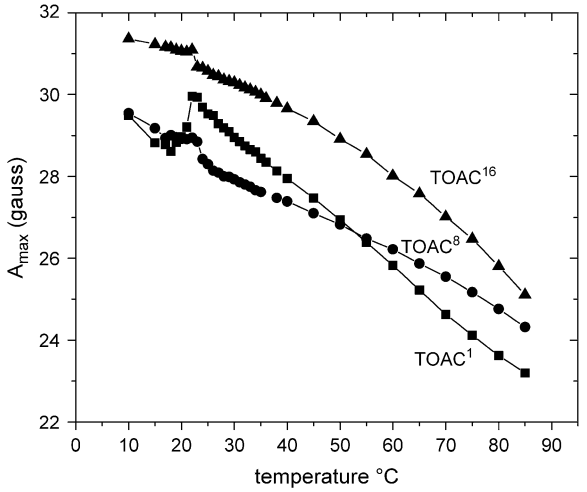

FIGURE 2 Temperature dependence of the outer hyperfine splitting constant, A_{max}, for [Glu(OMe)^{7,18,19}] alamethicin TOAC^1 (*squares*), TOAC^8 (*circles*), and TOAC^{16} (*triangles*) analogs in DMPC bilayers.

apparently anomalous. The mean values of the isotropic hyperfine couplings are: $a_o = 15.41 \pm 0.01$ G, 15.01 ± 0.01 G, and 15.03 ± 0.07 G, for the TOAC^1, TOAC^8, and TOAC^{16} analogs, respectively. The lower values indicate that the TOAC^8 and TOAC^{16} analogs are situated considerably deeper in the hydrophobic core of the membrane than is the TOAC^1 analog. For the TOAC^{16} analog, only the values at higher temperature were taken and are associated with a higher uncertainty, as indicated. For a TOAC peptide in water, the isotropic hyperfine coupling is considerably higher: $a_o =$ 16.2–16.5 G, depending on the pH/charge state of the peptide (40). This implies that the TOAC^1 analog is not directly exposed to water, but is probably located close to the polar-apolar interface of the membrane, as suggested also for surface-associated trichogin GA IV and melanocortin (41,42). Note that a higher water exposure of TOAC^1 than of TOAC^{16} (at high temperature) does not exclude the possibility of a yet greater water exposure of a spin label attached to the C-terminal phenylalaninol, especially at lower temperatures (43).

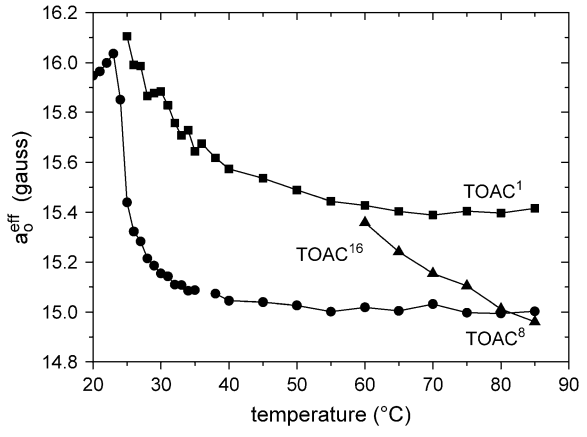

FIGURE 3 Temperature dependence of the effective isotropic hyperfine couplings, a_o, for [Glu(OMe)^{7,18,19}] alamethicin TOAC^1 (*squares*), TOAC^8 (*circles*), and TOAC^{16} (*triangles*) analogs in DMPC bilayers.

Orientational order parameters

Fig. 4 gives the temperature dependence of the order parameters, S_{zz}, for the three TOAC analogs of alamethicin in DMPC bilayer membranes in the fluid phase. According to the criterion of constant a_o, the data in Fig. 3 suggest that motional narrowing theory should be applicable above 55°C for all except the TOAC^{16} analog. As already noted, the spectra are axially symmetric in this temperature regime (see Fig. 1). The values given in Fig. 4 therefore should be reasonably representative of the time-average angular amplitude of the spin-label z axis, relative to the director for the uniaxial rotational motion. At temperatures below those for which data is given in Fig. 4, motional narrowing theory can no longer be relied upon for determining order parameters.

Fig. 5 shows the conventional EPR spectra of the three TOAC-containing analogs of alamethicin in aligned multibilayers of fully hydrated DMPC in the fluid phase. Spectra are shown for the static magnetic field parallel (*solid lines*) and perpendicular (*dashed lines*) to the normal to the orienting quartz substrate on which the multibilayers are deposited. Although the degree of alignment of the sample is probably not completely homogeneous, and at these temperatures (30–32°C) the rotational motion is not yet in the fast regime (especially for the TOAC^{16} analog), there is clear anisotropy between spectra recorded with the parallel and perpendicular orientations of the magnetic field. For all three TOAC positions, the largest hyperfine splitting of the first derivative-like

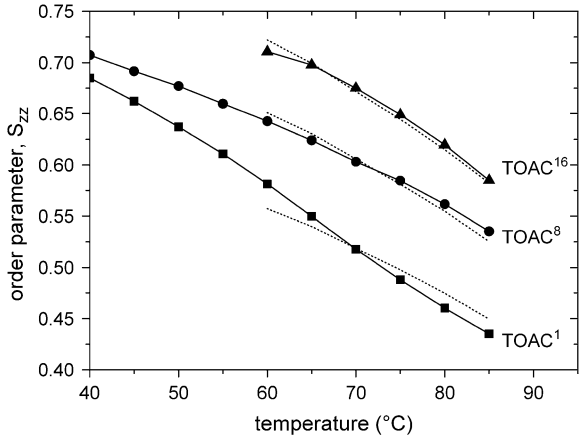

FIGURE 4 Temperature dependence of the effective order parameters, S_{zz}, for [Glu(OMe)^{7,18,19}] alamethicin TOAC^1 (*squares*), TOAC^8 (*circles*), and TOAC^{16} (*triangles*) analogs in DMPC bilayers. Solid lines are experimental measurements; dotted lines are a nonlinear least-squares fit of Eq. 6 to the temperature dependence, with constant θ_z for each TOAC position (see text and Fig. 6).

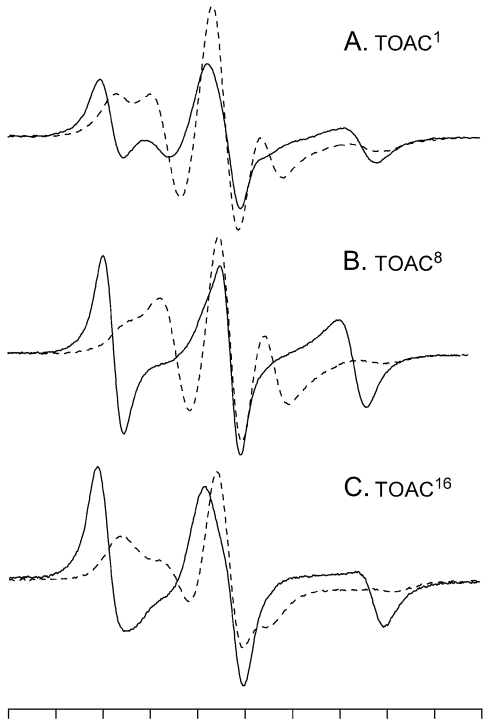

FIGURE 5 Conventional V_1-EPR spectra of [$TOAC^n$, $Glu(OMe)^{7,18,19}$] alamethicin analogs in aligned DMPC bilayers. (*Solid lines*, magnetic field parallel to the membrane normal; *dashed lines*, magnetic field perpendicular to the membrane normal.) (*A*) $TOAC^1$-alamethicin at 30°C; (*B*) $TOAC^8$-alamethicin at 32°C; and (*C*) $TOAC^{16}$-alamethicin at 32°C. Total scan width = 100 Gauss.

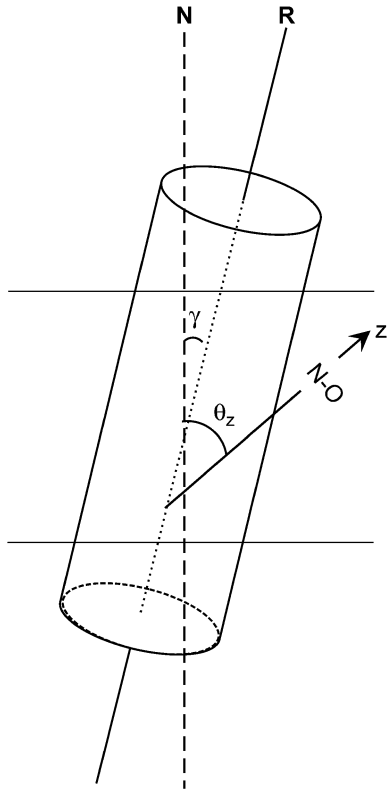

FIGURE 6 Orientation of TOAC-labeled alamethicin in a lipid membrane. The principal molecular diffusion axis, **R**, is inclined at instantaneous angle γ to the membrane normal **N**. The nitroxide z axis is oriented at constant angle θ_z to **R**. The experimental order parameter, S_{zz}, of the nitroxide z axis is given by Eq. 6, where, for axial symmetry, $\langle P_2(\cos\gamma)\rangle$ is the order parameter of the alamethicin diffusion axis.

single absorption lines is obtained in the parallel orientation with the magnetic field lying along the substrate normal (see, e.g., (14)). This finding confirms that the director, **N**, for the uniaxial rotation lies along the membrane normal, consistent with a transmembrane orientation of the alamethicin molecule as indicated by the isotropic hyperfine couplings.

For uniaxial motional averaging, the EPR order parameter of TOAC is given by the addition theorem for spherical harmonics,

$$S_{zz} = \langle P_2(\cos\gamma)\rangle \times P_2(\cos\theta_z), \tag{6}$$

where γ is the angle that the principal rotational diffusion axis, **R**, of the TOAC-labeled alamethicin molecule makes with the membrane normal, **N**, and θ_z is the inclination of the spin-label z axis to **R** (see Fig. 6). $P_2(x) = (3x^2-1)/2$ is a second-order Legendre polynomial and the angular brackets indicate a time average over the rotational motion. Because the TOAC spin label is rigidly attached to the peptide backbone, the different values of S_{zz} in Fig. 4 imply different orientations, θ_z, of the three TOAC residues to **R**. The crystal structure of native alamethicin reveals an α-helical conformation that is bent (31). This bend, together with local distortions, could account for the dependence of the TOAC order parameters on residue position.

The dotted lines in Fig. 4 represent a nonlinear least-squares fit of Eq. 6 to the temperature dependence of S_{zz} for all three TOAC labels, under the assumption that the spin-label inclination to the diffusion axis is temperature-independent. The order parameter of the diffusion axis, relative to **N**, then varies from $\langle P_2(\cos\gamma)\rangle = 0.87$–$0.70$ over the temperature range 60–85°C. The local orientation of the individual spin labels is characterized by the fixed values $\theta_z =$ 30°, 25°, and 20° for $TOAC^1$, $TOAC^8$, and $TOAC^{16}$, respectively. Judging from the goodness of the fits in Fig. 4, only for $TOAC^1$ are there significant changes in θ_z with temperature, possibly corresponding to a local unwinding of the helix or other conformational reorientation at the first residue position.

TOAC orientation in alamethicin

Fig. 7 shows one of the molecules (A) in the crystal structure of native alamethicin (31) into which the crystal structure of the TOAC moiety from molecule B of *Z*-TOAC-(L-Ala)$_2$-NH*t*Bu (29) has been incorporated at residue position 1, 8, or 16. This was done by constraining the coordinates of the

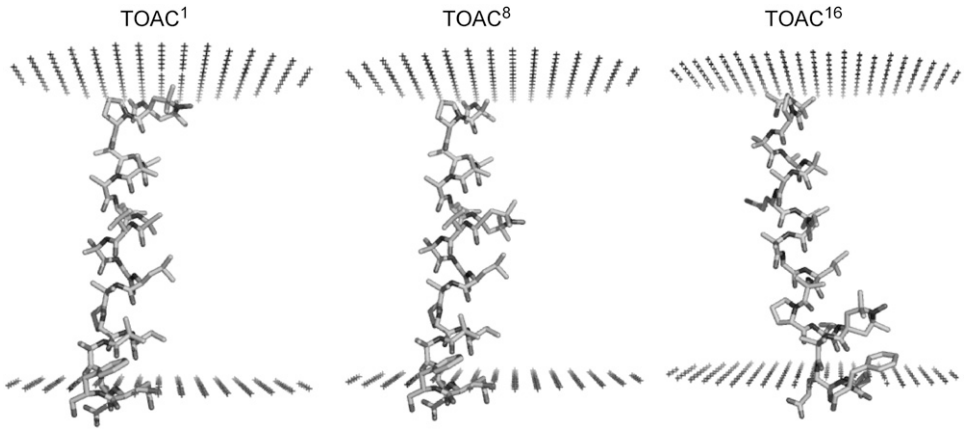

FIGURE 7 Crystal structure for molecule A of native alamethicin ((31); PDB: 1amt) with the TOAC structure from molecule B of Z-TOAC-(L-Ala)$_2$-NH*t*Bu ((29) CCDC: 123753) substituted for Aib at residue position 1, 8, or 16. The alamethicin molecule is oriented relative to the membrane surfaces as predicted in the OPM database (53).

TOAC N, C^{α}, and C′ atoms to coincide with those of Aib^1, Aib^8, or Aib^{16} in alamethicin. If the axis of the longer helical segment is defined as the line that is equidistant from the C^{α} atoms of residues 4–14, the inclination of the nitroxide *z* axis to this axis is $\theta_{\alpha} = 7°$, 15°, and 34°, for TOAC at residue positions 1, 8, and 16, respectively. For the recently solved structure of [$TOAC^{16}$, $Glu(OMe)^{7,18,19}$] alamethicin (33), the orientation of the spin-label *z* axis to the longer helical axis is $\theta_{\alpha} = 10$–12° and, for this TOAC structure grafted at residue positions 1 and 8, is $\theta_{\alpha} = 4$–7° and 8–9°, respectively. In terms of residue position, these values for the TOAC orientation θ_{α} are in the opposite order to those of θ_z that are derived from the EPR results. From this, one must conclude that the diffusion axis does not coincide with the helical axis between residues 4 and 14, as defined above. Taking the more recent crystal structure, the rotation axis **R** is tilted relative to the principal helix axis by ~30°. This value may be somewhat of an upper estimate because of the effects of local helix distortions that were referred to above. Note that taking the mirror-image $^2T_6$ twist-boat conformer of TOAC would predict nitroxide *z*-axis orientations that are incompatible with the EPR order-parameter measurements (30,44).

Saturation transfer spin-label EPR spectra

Fig. 8 shows the saturation transfer EPR spectra of the three different $TOAC^1$, $TOAC^8$, and $TOAC^{16}$ analogs of [$Glu(OMe)^{7,18,19}$] alamethicin in DMPC bilayer membranes. Spectra are shown at various temperatures, both above and below the lipid chain-melting temperature of 23°C. The spectra are scaled to line height, rather than to the absolute intensity, which decreases with increasing temperature. In the gel phase, the ST-EPR spectra have appreciable intensity, not only in the overall spectrum, but also in the diagnostic regions at intermediate positions in the low-, high-, and center-field manifolds of the ^{14}N-hyperfine structure. These nonvanishing ST-EPR intensities reflect the response of the peptide to the extremely slow rotational diffusion of the gel-phase lipids, with effective correlation times beyond the microsecond regime (45,46). Immediately above the lipid chain-melting transition, the overall intensity of the ST-EPR spectrum drops abruptly and the spectral lineshape changes because of preferential reduction in the line heights at the diagnostic L″, C′, and H″ positions relative to the stationary turning points at positions L, C and H, respectively (see, e.g., (15)). These spectra are characteristic of very fast motion, no longer in the microsecond regime (at least for the central C′ region of the spectrum), and reflect the response of the peptide mobility to the rapid lipid chain motions in the fluid membrane phase (45,47).

Fig. 9 gives the temperature dependence of the normalized ST-intensity, I_{ST}, and the diagnostic line-height ratios, L″/L, C′/C, and H″/H, for the $TOAC^8$ alamethicin analog in DMPC membranes. This is the analog with highest ST-EPR intensities and, therefore, that most likely to exhibit any microsecond motions that are associated with the whole peptide. All four ST-EPR parameters clearly reflect the change in overall peptide dynamics at the gel-fluid phase transition, which occurs at ~23°C. The values of the C′/C line-height ratio and of the ST integral are very low in the fluid phase, beyond those for which ST-EPR calibrations were made. This corresponds to an effective rotational correlation time of $<2.9 \times 10^{-8}$ s (28). In addition, the L″/L ratio is seen to increase with increasing temperature, i.e., with decreasing correlation time. This is a feature of incipient motional narrowing in ST-EPR spectra (15), that again is consistent with correlation times of $<10^{-7}$ s. Such rapid rotational reorientation suggests rather strongly that the peptide is not aggregated in fluid DMPC membranes, as was concluded already from the lack of spin-spin broadening of the conventional EPR spectra. Standard hydrodynamic theory (see, e.g., (48)) predicts a rotational correlation time of 1.4–2.8×10^{-7} s for a single transmembrane α-helix in a membrane of effective viscosity 2.5–5 P (49). For a dimer, this value increases to 3.5–7.0×10^{-7} s, and for a tetramer to 5.6–11.3×10^{-7} s. It therefore seems most likely that the TOAC alamethicin analogs are monomeric (at a concentration

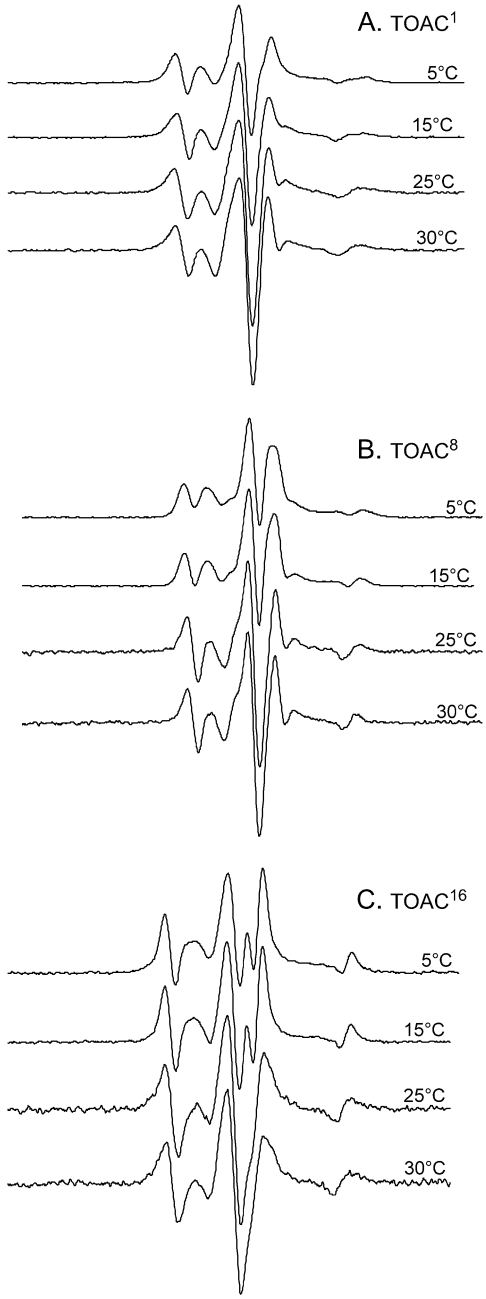

FIGURE 8 Saturation transfer EPR spectra (V_2'-display) of [Glu(OMe)^{7,18,19}] alamethicin analogs with TOAC substituted for (*A*) residue 1, TOAC^1; (*B*) residue 8, TOAC^8; and (*C*) residue 16, TOAC^{16}, in DMPC bilayers at the temperatures indicated. Total scan width = 160 Gauss.

of 1 mol %) in fluid DMPC bilayers, as suggested previously for alamethicin in vesicles of unsaturated phosphatidylcholines (35,36). Note that substitution of Gln residues, particularly the conserved Gln^7, by Glu(OMe) might reduce somewhat the propensity of alamethicin to form pores, as suggested by the lower conductance (18).

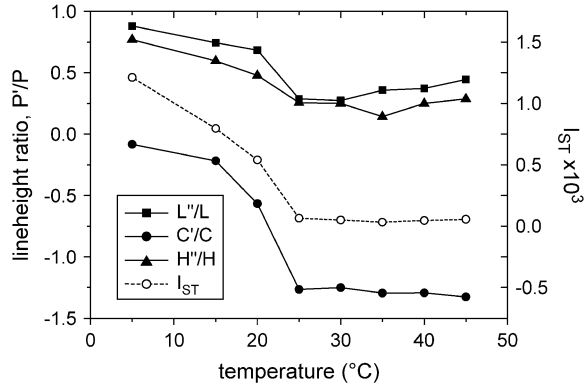

FIGURE 9 Temperature dependence of the integrated intensity, I_{ST} (*open circles*), and diagnostic line-height ratios, L′′/L (*squares*), C′/C (*solid circles*), and H′′/H (*triangles*), from the ST-EPR spectra of [TOAC^8, Glu(OMe)^{7,18,19}] alamethicin in DMPC bilayers.

CONCLUSIONS

The results from aligned samples and from the relative polarities of the environments of the different TOAC positions demonstrate that Glu(OMe)^{7,18,19} alamethicin adopts a transmembrane orientation in fluid bilayer membranes of DMPC. This is in agreement with other spectroscopic studies on unmodified and chemically labeled alamethicins (43,50). Certain models for the induction of ion channels propose a switching of the alamethicin long-axis from a surface to a transmembrane orientation (see, e.g., (2)). The present results show that the bulk of the peptide has a transmembrane orientation and therefore such channels are most likely formed by self-assembly within the membrane.

The combined order parameter measurements from the different TOAC positions indicate that the tilt of the long axis of the peptide, relative to the membrane normal, is fairly small with values of $\langle P_2(\cos\gamma)\rangle$ corresponding to effective tilt angles of 17–27° over the temperature range 60–85°C. It is expected that the tilt of alamethicin is restricted because the length of the molecule (~29 Å from C^α of residue 1 to C^α of residue 19) is relatively short compared with the thickness of a DMPC bilayer. For the latter, the hydrophobic thickness is ~26 Å and the total thickness is ~37 Å at 30°C, which extrapolate to 21 Å and 30 Å, respectively, at 85°C using an expansion coefficient of −0.004 per degree (51). Orientation of alamethicin according to the distribution of polarity/hydrophobicity in the molecule, as reported in the OPM database (see Fig. 7), predicts a transmembrane alignment of alamethicin with a hydrophobic depth of 28 Å and a tilt of 16 ± 8° (52,53). This theoretical prediction is therefore essentially in accord with the present experimental measurements.

An interesting feature of the angular motion of the TOAC spin labels, relative to that of spin-labeled lipid chains (see, e.g., (54)), is that the rotational diffusion is slow on the EPR timescale (~ns) in fluid membranes, except at rather high

temperatures (>60°C). This reflects the rigidity of the helical backbone of alamethicin and the anchoring of the TOAC ring at the C^{α}-position of the helix.

On the longer (μs) timescale of ST-EPR, however, rotation about the long axis of alamethicin is relatively rapid. This means that alamethicin is not forming large pore aggregates, which would have rotational correlation times in the microsecond regime. Most likely, the bulk of the alamethicin is monomeric in the fluid membrane, and pore formation (and growth) occurs via transient association of the monomeric species. This is in accordance with the electrophysiological channel behavior and proposals from other spectroscopic studies (43).

We thank Frau B. Angerstein and Frau B. Freyberg for skillful technical assistance, Dr. Marco Crisma for providing the coordinates of [$TOAC^{16}$, $Glu(OMe)^{7,18,19}$] alamethicin, and Frau I. Dreger for help with preparing Fig. 7.

REFERENCES

1. Nagaraj, R., and P. Balaram. 1981. Alamethicin, a transmembrane channel. *Acc. Chem. Res.* 14:356–362.
2. Sansom, M. S. 1991. The biophysics of peptide models of ion channels. *Prog. Biophys. Mol. Biol.* 55:139–235.
3. Gordon, L. G. M., and D. A. Haydon. 1972. The unit conductance channel of alamethicin. *Biochim. Biophys. Acta.* 255:1014–1018.
4. Boheim, G., and H.-A. Kolb. 1978. Analysis of the multi-pore system of alamethicin in a lipid membrane. I. Voltage-jump current-relaxation measurements. *J. Membr. Biol.* 38:99–150.
5. Opsahl, L. R., and W. W. Webb. 1994. Transduction of membrane tension by the ion-channel alamethicin. *Biophys. J.* 66:71–74.
6. Keller, S. L., S. M. Bezrukov, S. M. Gruner, M. W. Tate, I. Vodyanoy, and V. A. Parsegian. 1993. Probability of alamethicin conductance states varies with nonlamellar tendency of bilayer phospholipids. *Biophys. J.* 65:23–27.
7. Nakaie, C. R., G. Goissis, S. Schreier, and A. C. M. Paiva. 1981. pH-dependence of electron paramagnetic resonance spectra of nitroxides containing ionizable groups. *Braz. J. Med. Biol. Res.* 14:173–180.
8. Nakaie, C. R., S. Schreier, and A. C. M. Paiva. 1983. Synthesis and properties of spin-labeled angiotensin derivatives. *Biochim. Biophys. Acta.* 742:63–71.
9. Marchetto, R., S. Schreier, and C. R. Nakaie. 1993. A novel spin-labeled amino acid derivative for use in peptide synthesis—(9-fluorenylmethyloxycarbonyl)-2,2,6,6-tetramethylpiperidine-*N*-oxyl-4-amino-4-carboxylic acid. *J. Am. Chem. Soc.* 115:11042–11043.
10. Toniolo, C., M. Crisma, and F. Formaggio. 1998. TOAC, a nitroxide spin-labeled, achiral C^{α}-tetrasubstituted α-amino acid, is an excellent tool in materials science and biochemistry. *Biopolymers.* 47:153–158.
11. Karim, C. B., T. L. Kirby, Z. Zhang, Y. Nesmelov, and D. D. Thomas. 2004. Phospholamban structural dynamics in lipid bilayers probed by a spin label rigidly coupled to the peptide backbone. *Proc. Natl. Acad. Sci. USA.* 101:14437–14442.
12. Monaco, V., F. Formaggio, M. Crisma, C. Toniolo, P. Hanson, and G. L. Millhauser. 1999. Orientation and immersion depth of a helical lipopeptaibol in membranes using TOAC as an ESR probe. *Biopolymers.* 50:239–253.
13. Marsh, D. 2001. Polarity and permeation profiles in lipid membranes. *Proc. Natl. Acad. Sci. USA.* 98:7777–7782.
14. Schreier-Muccillo, S., D. Marsh, H. Dugas, H. Schneider, and I. C. P. Smith. 1973. A spin probe study of the influence of cholesterol on motion and orientation of phospholipids in oriented multibilayers and vesicles. *Chem. Phys. Lipids.* 10:11–27.
15. Thomas, D. D., L. R. Dalton, and J. S. Hyde. 1976. Rotational diffusion studied by passage saturation transfer electron paramagnetic resonance. *J. Chem. Phys.* 65:3006–3024.
16. Jost, M., C. Peggion, F. Formaggio, and C. Toniolo. 2006. Total synthesis in solution and preliminary conformational analysis of TOAC-labeled alamethicin F50/5 analogues. *In* Understanding Biology Using Peptides. S. E. Blondelle, editor. American Peptide Society, Secaucus, NJ. 263–264.
17. Peggion, C., I. Coin, and C. Toniolo. 2004. Total synthesis in solution of alamethicin F50/5 by an easily tunable segment condensation approach. *Biopolymers.* 76:485–493.
18. Baldini, C., C. Peggion, C. Toniolo, N. Vedovato, and G. Rispoli. 2007. Biophysical properties of alamethicin F50/5 and selective analogues inserted in rod outer segment membranes. *In* Peptides 2006. K. Rolka, editor. Kenes International, Geneva. In press.
19. Fajer, P., and D. Marsh. 1982. Microwave and modulation field inhomogeneities and the effect of cavity Q in saturation transfer ESR spectra. Dependence on sample size. *J. Magn. Reson.* 49:212–224.
20. Hemminga, M. A., P. A. De Jager, D. Marsh, and P. Fajer. 1984. Standard conditions for the measurement of saturation transfer ESR spectra. *J. Magn. Reson.* 59:160–163.
21. Rama Krishna, Y. V. S., and D. Marsh. 1990. Spin label ESR and ^{31}P-NMR studies of the cubic and inverted hexagonal phases of dimyristoylphosphatidylcholine/myristic acid (1:2, mol/mol) mixtures. *Biochim. Biophys. Acta.* 1024:89–94.
22. Schorn, K., and D. Marsh. 1996. Lipid chain dynamics and molecular location of diacylglycerol in hydrated binary mixtures with phosphatidylcholine: spin label ESR studies. *Biochemistry.* 35:3831–3836.
23. Schorn, K., and D. Marsh. 1997. Extracting order parameters from powder EPR lineshapes for spin-labeled lipids in membranes. *Spectrochim. Acta* [*A*]. 53:2235–2240.
24. Ondar, M. A., O. Ya. Grinberg, A. A. Dubinskii, and Ya. S. Lebedev. 1985. Study of the effect of the medium on the magnetic-resonance parameters of nitroxyl radicals by high-resolution EPR spectroscopy. *Sov. J. Chem. Phys.* 3:781–792.
25. Horváth, L. I., and D. Marsh. 1983. Analysis of multicomponent saturation transfer ESR spectra using the integral method: application to membrane systems. *J. Magn. Reson.* 54:363–373.
26. Marsh, D., and L. I. Horváth. 1992. A simple analytical treatment of the sensitivity of saturation transfer EPR spectra to slow rotational diffusion. *J. Magn. Reson.* 99:323–331.
27. Marsh, D. 1999. Spin label ESR spectroscopy and FTIR spectroscopy for structural/dynamic measurements on ion channels. *Methods Enzymol.* 294:59–92.
28. Horváth, L. I., and D. Marsh. 1988. Improved numerical evaluation of saturation transfer electron spin resonance spectra. *J. Magn. Reson.* 80: 314–317.
29. Flippen-Anderson, J. L., C. George, G. Valle, E. Valente, A. Bianco, F. Formaggio, M. Crisma, and C. Toniolo. 1996. Crystallographic characterization of geometry and conformation of TOAC, a nitroxide spin-labeled $C^{\alpha,\alpha}$-disubstituted glycine, in simple derivatives and model peptides. *Int. J. Pept. Protein Res.* 47:231–239.
30. Marsh, D. 2006. Orientation of TOAC amino-acid spin labels in α-helices and β-strands. *J. Magn. Reson.* 180:305–310.
31. Fox, R. O., Jr., and F. M. Richards. 1982. A voltage-gated ion channel model inferred from the crystal structure of alamethicin at 1.5 Å resolution. *Nature.* 300:325–330.
32. Berman, H. M., J. Westbrook, Z. Feng, G. Gilliland, T. N. Bhat, H. Weissig, I. N. Shindyalov, and P. E. Bourne. 2000. The protein data bank. *Nucleic Acids Res.* 28:235–242.
33. Crisma, M., F. Formaggio, M. Jost, C. Peggion, and C. Toniolo. 2005. Crystal structure of a spin-labeled alamethicin analogue. *In* 1st European Conference on Chemistry for Life Sciences: Understanding the Chemical Mechanisms of Life. Book of Abstracts, DCSB 234. Rimini, Italy.
34. Boheim, G., W. Hanke, and H. Eibl. 1980. Lipid phase transition in planar bilayer membrane and its effect on carrier- and pore-mediated ion transport. *Proc. Natl. Acad. Sci. USA.* 77:3403–3407.

35. Archer, S. J., J. F. Ellena, and D. S. Cafiso. 1991. Dynamics and aggregation of the peptide ion channel alamethicin. *Biophys. J.* 60: 389–398.

36. Barranger-Mathys, M., and D. S. Cafiso. 1994. Collisions between helical peptides in membranes monitored using electron paramagnetic resonance: evidence that alamethicin is monomeric in the absence of a membrane potential. *Biophys. J.* 67:172–176.

37. Marsh, D. 1981. Electron spin resonance: spin labels. *In* Membrane Spectroscopy. Molecular Biology, Biochemistry and Biophysics, Vol. 31. E. Grell, editor. Springer-Verlag, Berlin, Heidelberg, New York. 51–142.

38. Marsh, D. 2002. Membrane water-penetration profiles from spin labels. *Eur. Biophys. J.* 31:559–562.

39. Marsh, D. 2002. Polarity contributions to hyperfine splittings of hydrogen-bonded nitroxides—the microenvironment of spin labels. *J. Magn. Reson.* 157:114–118.

40. Schreier, S., S. R. Barbosa, F. Casallanovo, R. Vieira, E. M. Cilli, A. C. M. Paiva, and C. R. Nakaie. 2004. Conformational basis for the biological activity of TOAC-labeled angiotensin II and bradykinin: electron paramagnetic resonance, circular dichroism, and fluorescence studies. *Biopolymers.* 74:389–402.

41. Monaco, V., F. Formaggio, M. Crisma, C. Toniolo, P. Hanson, and G. Millhauser. 1999. Orientation and immersion depth of a helical lipopeptaibol in membranes using TOAC as an ESR probe. *Biopolymers.* 50:239–253.

42. Fernandez, R. M., R. F. F. Vieira, C. R. Nakaie, M. T. Lamy, and A. S. Ito. 2005. Acid-base titration of melanocortin peptides: evidence of Trp rotational conformer interconversion. *Biopolym. Pept. Sci.* 80:643–650.

43. Barranger-Mathys, M., and D. S. Cafiso. 1996. Membrane structure of voltage-gated channel forming peptides by site-directed spin-labeling. *Biochemistry.* 35:498–505.

44. Hanson, P., D. J. Anderson, G. Martinez, G. Millhauser, F. Formaggio, M. Crisma, C. Toniolo, and C. Vita. 1998. Electron spin resonance and structural analysis of water soluble, alanine-rich peptides incorporating TOAC. *Mol. Phys.* 95:957–966.

45. Marsh, D. 1980. Molecular motion in phospholipid bilayers in the gel phase: long axis rotation. *Biochemistry.* 19:1632–1637.

46. Fajer, P., A. Watts, and D. Marsh. 1992. Saturation transfer, continuous wave saturation, and saturation recovery electron spin resonance studies of chain-spin labeled phosphatidylcholines in the low temperature phases of dipalmitoyl phosphatidylcholine bilayers. Effects of rotational dynamics and spin-spin interactions. *Biophys. J.* 61:879–891.

47. Bartucci, R., T. Páli, and D. Marsh. 1993. Lipid chain motion in an interdigitated gel phase: conventional and saturation transfer ESR of spin-labeled lipids in dipalmitoylphosphatidylcholine-glycerol dispersions. *Biochemistry.* 32:274–281.

48. Marsh, D., and L. I. Horváth. 1989. Spin-label studies of the structure and dynamics of lipids and proteins in membranes. *In* Advanced EPR. Applications in Biology and Biochemistry. A. J. Hoff, editor. Elsevier, Amsterdam, The Netherlands. 707–752.

49. Cherry, R. J., and R. E. Godfrey. 1981. Anisotropic rotation of bacteriorhodopsin in lipid membranes. *Biophys. J.* 36:257–276.

50. Vogel, H. 1987. Comparison of the conformation and orientation of alamethicin and melittin in lipid membranes. *Biochemistry.* 26: 4652–4672.

51. Nagle, J. F., and S. Tristram-Nagle. 2000. Structure of lipid bilayers. *Biochim. Biophys. Acta.* 1469:159–195.

52. Lomize, A. L., I. D. Pogozheva, M. A. Lomize, and H. I. Mosberg. 2006. Positioning of proteins in membranes: a computational approach. *Protein Sci.* 15:1318–1333.

53. Lomize, M. A., A. L. Lomize, I. Pogozheva, and H. I. Mosberg. 2006. OPM: orientations of proteins in membranes database. *Bioinformatics.* 22:623–625.

54. Schorn, K., and D. Marsh. 1996. Lipid chain dynamics in diacylglycerol-phosphatidylcholine mixtures studied by slow-motional simulations of spin label ESR spectra. *Chem. Phys. Lipids.* 82:7–14.